Measuring Magnetization Reversal in Antidot Arrays by Using X-ray Magnetic Circular Dichroism

D.R. Lee,[1] Y. Choi,[1] J.C. Lang,[1] D. Haskel,[1] G. Srajer,[1] V. Metlushko[2]
[1]Advanced Photon Source (APS), Argonne National Laboratory, Argonne, IL, U.S.A.
[2]Department of Electrical and Computer Engineering, University of Illinois at Chicago, IL, U.S.A.

Introduction

Antidot (hole) arrays in continous magnetic films have recently received much attention because of their potential advantages over magnetic dot array systems for data storage [1]. Two advantages are (1) there is no superparamagnetic lower limit to the bit size and (2) the intrinsic properties of the continuous magnetic film are preserved. Antidot arrays possess unique magnetic properties, such as their shape-induced magnetic anisotropy, domain structure, and pinning in laterally confined geometries. Typically, antidot arrays at remanence show three types of domains behaving collectively as single domains [2].

Domain formation at remanence is understood to be mainly the result of the interplay between the intrinsic anisotropy and the shape anisotropy due to the antidots [1, 2]. The coexistence of well-defined domains with individual magnetizations provides an opportunity to study the energetics between domains during magnetic switching. Here we present x-ray magnetic circular dichorism (XMCD) as a vector magnetometry (VM) to understand the switching mechanism in antidot arrays. The approach is complementary to previous microscopy studies [2]. This work is also important for future studies of the interlayer coupling under lateral confinement, because the element-specific XMCD technique is ideally suited for heteromagnetic systems such as Gd/Fe multilayers.

Methods and Materials

For the VM studies, hysteresis loops were measured by recording XMCD signals. Because XMCD is proportional to the projection of the magnetization vector **M** along the photon momentum direction $\mathbf{k}_{ph}$ near resonance energies [i.e., XMCD is proportional to $\mathbf{k}_{ph}.\mathbf{M} = \cos\gamma$, as shown in the inset of Fig. 1(a)], this technique allows element-specific determination of the orientation of the average magnetization. This is done by collecting hysteresis curves with more than two orthogonal incident photon directions for a given field [3].

Multilayered $[Fe\ (3\ nm)/Gd\ (2\ nm)]_8$ films were prepared on Si substrates by e-beam deposition. Square arrays of circular holes with a period of 2 μm and a diameter of 1 μm were generated by using standard lithography and liftoff processes. Magneto-optic Kerr effect (MOKE) hysteresis loops were measured for both unpatterned and patterned films to determine the direction of intrinsic uniaxial magnetic anisotropy. The XMCD measurements were performed at SRI-CAT beamline station 4-ID-D at the APS. Circularly polarized hard x-rays were produced by a diamond (111) quarter-wave plate operated in Bragg transmission geometry [4]. The XMCD effects were measured in fluorescence around the Fe K absorption edge (7.111 keV) by switching the helicity of the incident radiation. For the vector magnetometry studies, the sample/electromagnet assembly was rotated with respect to the projected incident photon direction.

Results and Discussion

Figure 1 shows XMCD hysteresis loops measured with four different directions of incident x-ray beams. ϕ = (a) 0°, (b) −45°, (c) −90°, and (d) −135° with respect to the field applied in the positive direction. While $\phi = 0°$ corresponds to the conventional hysteresis loop along the applied field direction, the rotation of the average magnetization of the sample at $\phi = -90°$ can be described by $\theta_{avg} = -\tan^{-1}(M_{-90}/M_0)$. This was surprising because many domains were expected to form. Following this relationship, one can determine a counterclockwise rotation of magnetization from Fig. 1(a) and 1(c) induced by the easy axis orientation of the intrinsic uniaxial anisotropy, as depicted by the inset in Fig. 1(a). The preferential rotation gives rise to a dramatic asymmetry between the $\phi = -45°$ and $\phi = -135°$ loops. Interestingly, $\phi = -45°$ hysteresis shows three loops whose tie points correspond to the coercive fields.

Since XMCD-VM measures a spatially averaged magnetization, numerical micromagnetic simulations have been performed to reconstruct the microscopic domain configuration. The hysteresis loops were calculated by using micromagnetic simulations and were fitted to the experimental data from XMCD-VM by varying the uniaxial anisotropy, exchange stiffness, and saturation magnetization as parameters. The fitted results from the 2-D code are shown as solid lines in Fig. 1 and are in good agreement with the measured XMCD hysteresis loops. The reconstructed spin configurations with the best-fit parameters clearly showed three main types of domains, as reported previously [2].

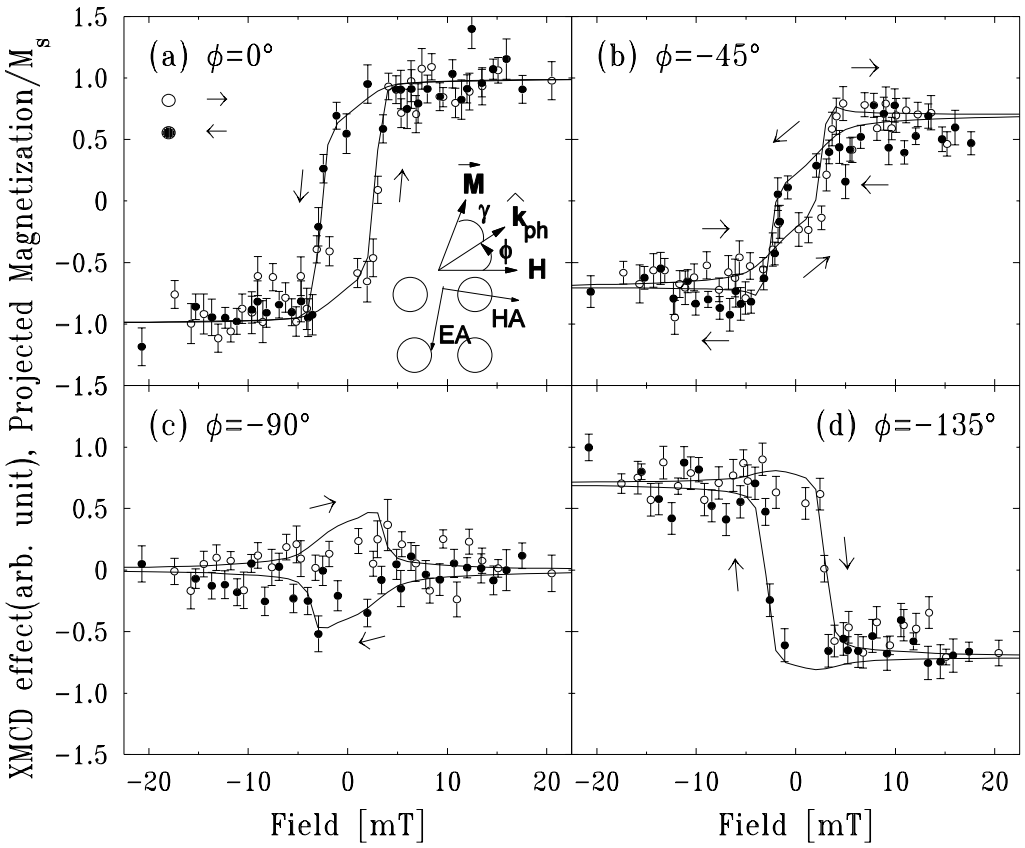

FIG. 1. XMCD magnetic hysteresis loops (circles) measured at the Fe K edge at room temperature. To obtain vector information on the average magnetization, the incident photon beams were rotated with respect to the positive field direction, by ϕ = (a) 0°, (b) –45°, (c) –90°, and (d) –135°. The inset in (a) shows a schematic of the experimental setup, where γ is the angle between the magnetization vector **M** and the incident photon momentum direction $\mathbf{k}_{ph}$, **H** is the applied field, and "EA" and "HA" denote the easy- and hard-axis of the intrinsic anisotropy, respectively. The solid lines represent the calculated hysteresis loops from using micromagnetic simulations.

A sequence of spin configurations reveals that two types of domains rotate coherently while one is pinned. To understand intuitively the coherent rotations, we have developed a simple phenomenological energy model by employing the Stoner-Wohlfarth single-domain model with an effective shape anisotropy. This model suggests that the interplay between the shape anisotropy and the intrinsic uniaxial anisotropy can explain the coherent rotations of domains as well as characteristic domain formations in antidot arrays. The details of this work are given in Ref. 5.

Acknowledgments

Use of the APS was supported by the U.S. Department of Energy, Office of Science, Office of Basic Energy Sciences, under Contract No. W-31-109-ENG-38.

References

[1] R.P. Cowburn, A.O. Adeyeye, and J.A.C. Bland, Appl. Phys. Lett. **70**, 2309-2311 (1997).

[2] A.Y. Toporov, R.M. Langford, and A.K. Petford-Long, Appl. Phys. Lett. **77**, 3063-3065 (2000).

[3] V. Chakarian, Y.U. Idzerda, G. Meigs, E.E. Chaban, J.-H. Park, and C.T. Chen, Appl. Phys. Lett. **66**, 3368-3370 (1995).

[4] J.C. Lang and G. Srajer, Rev. Sci. Instrum. **66**, 1540-1542 (1995).

[5] D.R. Lee, Y. Choi, C.-Y. You, J.C. Lang, D. Haskel, G. Srajer, V. Metlushko, B. Ilic, and S.D. Bader, Appl. Phys. Lett. **81**, 4997-4999 (2002).